

Lab on a Chip

Electronic Supplementary Information (ESI)

Integrating nanofibers with biochemical gradients to investigate physiologically-relevant fibroblast Chemotaxis

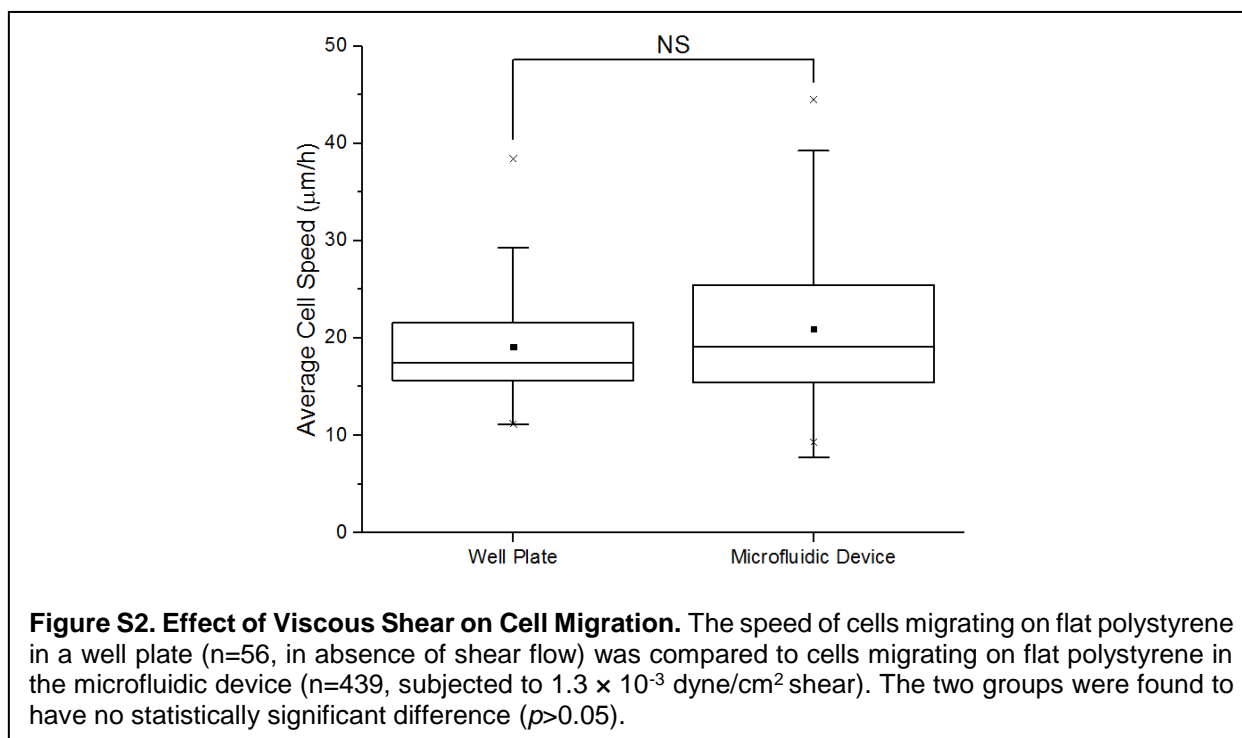
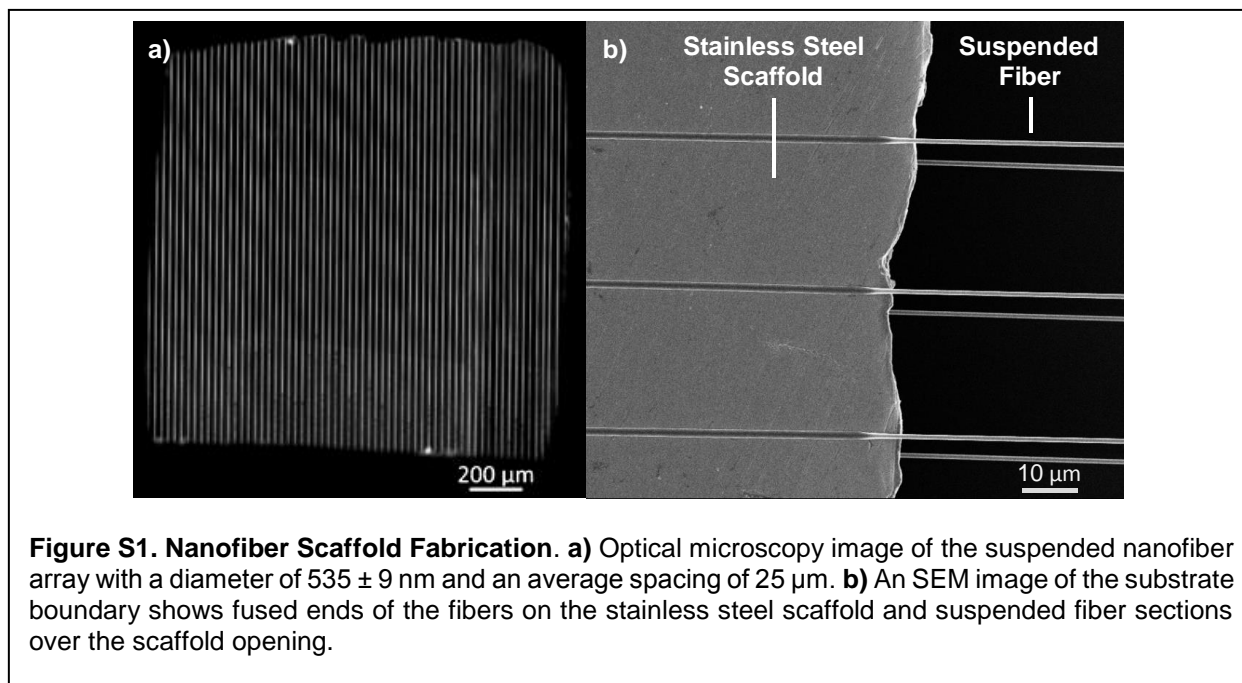
Carmen M. Morrow^a, Apratim Mukherjee^a, Mahama A. Traore^{a,b}, Eric J. Leaman^a, AhRam Kim^a,
Evan M. Smith^a, Amrinder S. Nain^{a,b}, Bahareh Behkam^{a,b,*}

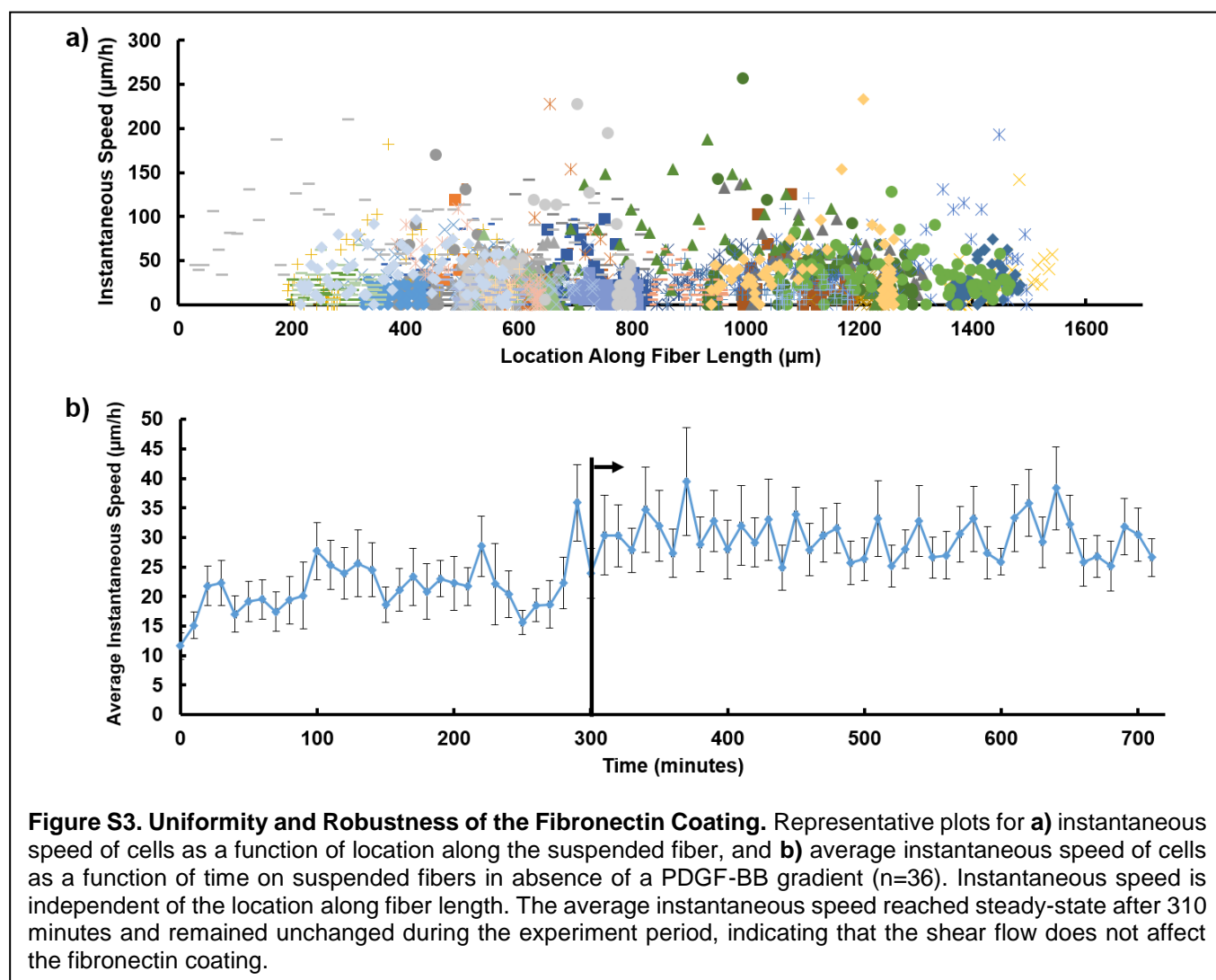
^a Department of Mechanical Engineering, Virginia Tech, Blacksburg, VA 24061, USA

^b School of Biomedical Engineering & Sciences, Virginia Tech, Blacksburg, VA 24061, USA

* Corresponding author: behkam@vt.edu

S.I. Supplementary Figures





S.II. Microfluidic Device Design

The microfluidic device used in this study has two inlets, one for a buffer solution and the other for the chemo-effector of interest, which feed into a network of diffusive mixing channels. Eleven channels exit from the serpentine diffusive mixing channels, each containing uniform chemical concentrations that are different from one channel to another, and converge into the main observation channel. As the laminar streams from these channels come into contact, diffusion across the streams leads to the development of a linear chemical gradient. In order to establish a linear chemical gradient over the majority of the observation channel length, the inlet flow rates need to be carefully designed. If the flow rate is very high, the eleven streams remain discrete, as there will not be enough time for molecular diffusion and interfacial mixing of the streams. If the flow rate is very low, too much mixing will occur, and there will be little to no chemical concentration gradient throughout the observation channel.

To determine the appropriate flowrate, the advection-diffusion equation for the chemical gradient in the observation channel was solved:

$$\frac{\partial c}{\partial t} + \nabla \cdot (\mathbf{v}c) - \nabla \cdot (D\nabla c) = sc \quad (\text{S-1})$$

where c is the concentration of the chemo-effector, D is the diffusion coefficient of the chemo-effector in the buffer solution, and s is the time rate of generation/degradation of the chemo-effector. The $\frac{\partial c}{\partial t}$ term represents the time rate of change in the chemo-effector concentration, $\nabla \cdot (vc)$ is the advective term due to fluid velocity, \mathbf{v} , and $-\nabla \cdot (D\nabla c)$ is the diffusive term. This equation was simplified based on the following assumptions: (1) the system is at steady-state, and therefore, there is no change in chemo-effector concentration over time; (2) there is no generation/degradation of the chemo-effector; (3) there is only advection in the y -direction (along the length of the channel), and transport due to diffusion in the y -direction is negligible when compared to convection. To ensure the last assumption is valid, the Peclet number, Pe , a non-dimensional term that compares the importance of convective and diffusive transport, was calculated

$$Pe = \frac{Lv}{D} \quad (\text{S-2})$$

where L is the characteristic length, which for this case is the hydraulic diameter for a rectangular cross-section.

$$L = \frac{2wh}{w+h} \quad (\text{S-3})$$

where w is the width of the channel, and h is the height of the channel. Using $v_y = 15 \mu\text{m/s}$, $D = 100 \mu\text{m}^2/\text{s}$, $w = 2200 \mu\text{m}$, $h = 500 \mu\text{m}$, the Peclet number is $Pe = 122$. Since $Pe \gg 1$, the assumption that convection dominates diffusion is indeed valid.

Based on the above three assumptions, equation S-1 can be simplified to

$$\frac{\partial c}{\partial y} = \frac{D}{v_y} \left(\frac{\partial^2 c}{\partial x^2} \right) \quad (\text{S-4})$$

For simplification purposes, v_y is assumed to be the average fluid velocity in the y -direction. This is a good assumption because the velocity varied only by 16.6% across the nanofiber length (**Figure S5**). The flow rate, Q , can be calculated by

$$Q = A_c v_y \quad (\text{S-5})$$

where A_c is the cross-sectional area of the observation channel.

A numerical model was developed in MATLAB to explicitly solve the simplified differential transport equation (Equation S-4). Briefly, a central finite difference formulation in x and y was written, and then an explicit scheme was set. The derived finite difference equation is

$$\frac{C_{i,j+1} - C_{i,j-1}}{2\Delta y} = \frac{D}{v_y} \frac{C_{i-1,j} - 2C_{i,j} + C_{i+1,j}}{\Delta x^2} \quad (\text{S-6})$$

with stability criteria of

$$0 \leq \frac{2D}{v_y} \frac{\Delta y}{\Delta x^2} \leq \frac{1}{2} \quad (\text{S-7})$$

The boundary conditions for the model are

$$\begin{aligned} c(x, 0) &= 0 \text{ for } 0 \leq x \leq 0.2 \text{ mm} \\ c(x, 0) &= .1C_0 \text{ for } 0.2 < x \leq 0.4 \text{ mm} \\ c(x, 0) &= .2C_0 \text{ for } 0.4 < x \leq 0.6 \text{ mm} \end{aligned} \quad (\text{S-8})$$

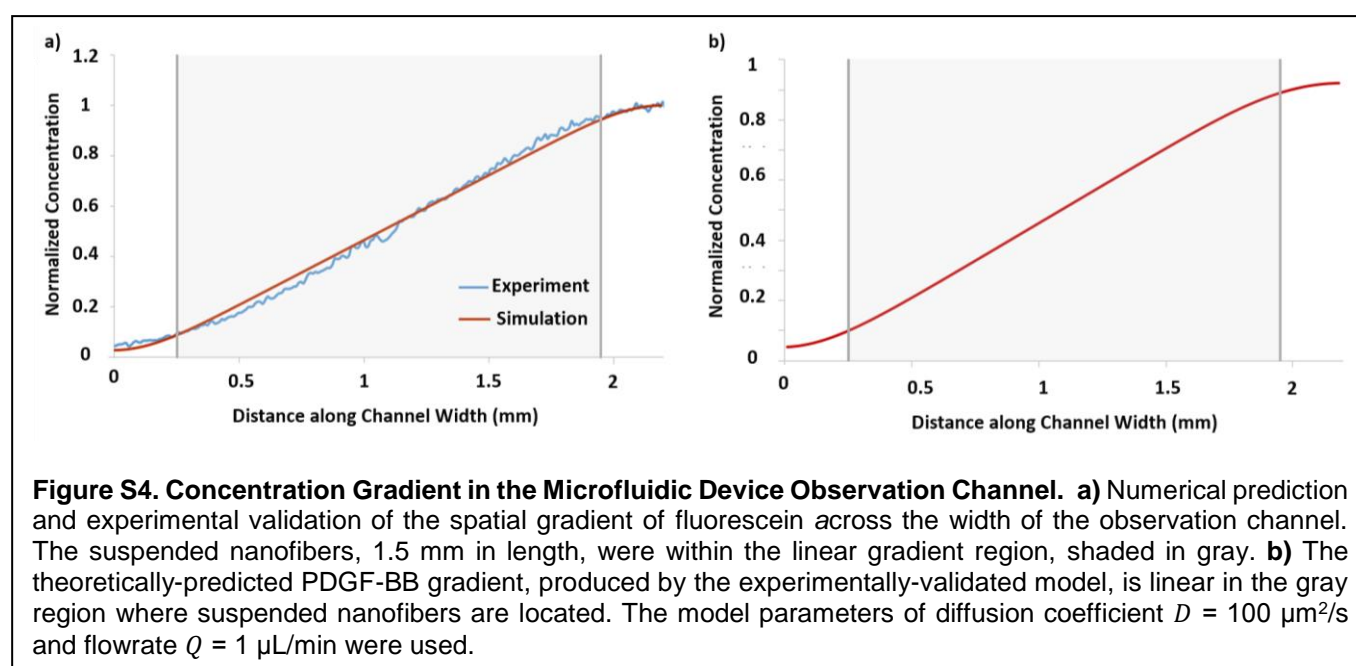
...

$$c(x, 0) = C_0 \text{ for } 2.0 < x \leq 2.2$$

$$\frac{\partial c}{\partial x} = 0 \text{ for } x = 0 \text{ and } x = 2.2 \text{ for all } y$$

where C_0 is the maximum chemo-effector concentration.

The numerical model explicitly solves for the spatial concentration gradient, as shown in **Figure S4a**. This model was then experimentally validated by flowing a 100 μM fluorescein solution in phosphate-buffered saline (PBS) and a PBS buffer solution through the inlets and measuring the fluorescent intensity profile in the observation channel. We confirmed that a linear gradient at the predicted flow rate could be established in the center region of the observation channel. When centered in the observation channel, the suspended nanofibers, which were 1.5 mm in length, were within the linear region of the chemical gradient. The diffusion coefficient used for fluorescein was 270 $\mu\text{m}^2/\text{s}$, and the predicted flowrate to generate a linear gradient was 4 $\mu\text{L}/\text{min}$. The computationally predicted, and the experimentally measured gradients are shown in Figure S4.



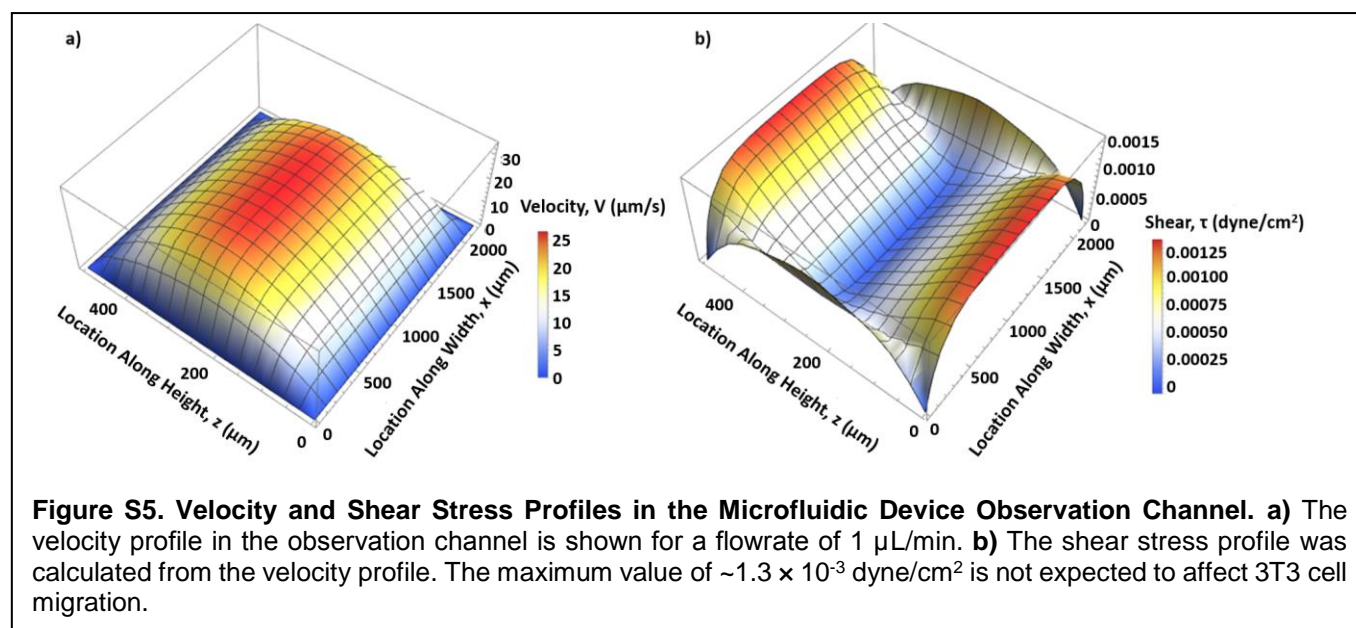
S.III. Analysis of the Fluid Flow

In flow-based microfluidic devices, effect of the shear stress generated by the flow on cell behavior must be considered. The fluid velocity and the shear stress profiles inside the observation channel were calculated to ensure that shear did not have significant effects. The Reynolds number (Re) using $v = 15 \mu\text{m}/\text{s}$ and $\nu = 1 \times 10^{-6} \mu\text{m}^2/\text{s}$ was calculated to be 1.2×10^{-2} . Since $Re \ll 1$, inertial effects were assumed to be negligible, compared to viscous effects. Therefore, for the steady-state fully developed viscous flow in the channel, the governing equations can be simplified to

$$\nabla p - \mu \nabla^2 \mathbf{v} = 0, \quad \nabla \cdot \mathbf{v} = 0 \quad (\text{S-9})$$

The solution of these simplified equations for a flow through a rectangular cross section channel yields the following equation for the fully developed fluid velocity, v_y .

$$v_y(x, z) = \frac{4h^2 \Delta p}{\pi^3 \mu L} \sum_{n=1,3,5,\dots}^{\infty} \frac{1}{n^3} \left[1 - \frac{\cosh\left(\frac{n\pi x}{h}\right)}{\cosh\left(\frac{n\pi w}{2h}\right)} \right] \sin\left(n\pi \frac{z}{h}\right) \quad (\text{S-10})$$



where z is the coordinate along the height of the channel, h , x is the coordinate along the width of the channel, w , y is the coordinate along the length of the channel, L , Δp is the pressure drop along the length of the channel, and μ is the dynamic viscosity of the fluid (assumed as the value of water). The pressure drop Δp can be calculated from

$$\Delta p = \frac{12Q\mu L}{wh^3} \left[1 - \sum_{n=1,3,5,\dots}^{\infty} \frac{1}{n^5} \frac{192}{\pi^5} \frac{h}{w} \tanh\left(n\pi \frac{w}{2h}\right) \right]^{-1}, \quad (\text{S-11})$$

where Q is the volumetric flowrate. The shear profile, τ , is then calculated by the following equation¹:

$$\tau = \mu \sqrt{\left(\frac{dv}{dx}\right)^2 + \left(\frac{dv}{dz}\right)^2} \quad (\text{S-12})$$

Using the experimental parameters, the velocity and shear profiles shown in **Figure S5** were generated. The maximum shear was located at the upper and lower walls of the observation channel and was approximately 1.3×10^{-3} dyne/cm² which is three orders of magnitude lower than the shear values reported to influence migration direction² and six orders of magnitude lower than the values reported to detach fibroblasts from a substrate³. Therefore, we assumed the shear had a negligible effect on cell behavior in these experiments. Furthermore, a set of experiments was conducted on flat polystyrene in well plates to quantify average 3T3 migration speed in CO₂-independent medium in the absence of any fluid shear. The average cell speed in the well plates (19.1 ± 5.5 $\mu\text{m}/\text{h}$, $n=56$) was compared to the average cell speed on flat polystyrene in the microfluidic device (20.9 ± 8.0 $\mu\text{m}/\text{h}$, $n=439$). There was no statistically significant difference between the two ($p > 0.05$), as shown in **Figure S2**.

References

- 1 F. M. White, *Viscous Fluid Flow*, McGraw-Hill, New York, 1974.
- 2 S. Song, H. Han, U. H. Ko, J. Kim and J. H. Shin, *Lab Chip*, 2013, **13**, 1602–1611.
- 3 H. Lu, L. Y. Koo, W. M. Wang, D. A. Lauffenburger, L. G. Griffith and K. F. Jensen, *Anal. Chem.*, 2004, **76**, 5257–5264.